# A Regime-Shift Index for Climate Monitoring

Thomas A. Weber
*Chair of Operations, Economics and Strategy*
*École Polytechnique Fédérale de Lausanne*
Lausanne, Switzerland
thomas.weber@epfl.ch

2026 International Conference on Sustainable Engineering and Digital Innovation (ICSEDI) | 979-8-3315-7563-2/26/$31.00 ©2026 IEEE | DOI: 10.1109/ICSEDI66420.2026.11568423

***Abstract*—Climate change manifests itself not only in shifts of long-run averages but also in changes to the entire distribution of environmental variables such as temperature, precipitation, and wind speed. This paper proposes a simple, rank-based *regime-shift index* (RSI) to quantify how much an observed climate regime departs from a reference distribution, such as a historical baseline or a policy target. The index compares cumulative distributions rather than densities and is therefore invariant under strictly increasing transformations of the underlying variable. Empirically, it can be estimated from daily or monthly data through a closed-form expression that depends only on the reference cumulative distribution function (CDF) evaluated at observed outcomes. We illustrate the method with a case study for Geneva–Cointrin (Switzerland), using homogeneous daily mean temperature data from 1864 to 2024 provided by MeteoSwiss. The regime-shift index is computed for successive decades relative to the 1961–1990 WMO normal period and summarizes the extent to which recent temperature distributions deviate from that baseline. The resulting one-number summaries complement standard climate indicators and yield clear, interpretable visualizations of regime shifts over time and across locations.**

***Keywords*—Climate change, climate indices, empirical distributions, environmental risk, regime shift, temperature distributions**

## I. Introduction

Climate systems are increasingly subject to stress from anthropogenic forcing, with impacts visible in the frequency and severity of heatwaves, droughts, storms, and other extremes [1]–[3]. While traditional climate indicators emphasize changes in mean temperature or total precipitation, the evolution of climate regimes is determined by the entire distribution of environmental variables. For example, two locations with identical mean temperature changes may differ dramatically in the probability of extreme events [4], [5].

This paper introduces a simple, distribution-based *regime-shift index* (RSI) to quantify the degree to which an observed climate regime differs from a reference distribution. The basic idea is to work at the level of cumulative distribution functions (CDFs), treating the observed regime as an unknown distribution $F$ and the baseline as a reference CDF $G$. A scalar index $R(F|G)$ is derived from the powered family of CDFs $\{G^r : r > 0\}$ and measures how much the reference distribution must be "tightened" or "loosened" to best approximate $F$ in an information-theoretic sense, in the spirit of the Kullback–Leibler divergence [6]. Operationally, $R(F|G)$ depends only on the values of $G$ at the observed outcomes, so it can be computed from empirical data without parametric assumptions or density estimation. Because $R(F|G)$ is defined relative to a chosen $G$, it is a *relative* regime-shift index.

From a practical standpoint, the proposed RSI supports three main tasks: (i) diagnosing shifts in climate regimes relative to a historical baseline, (ii) comparing the degree of regime shift of different regions or time periods on a common scale, and (iii) producing compact visual summaries of regime-shift trajectories. We demonstrate these ideas using daily temperature data from the Swiss National Basic Climatological Network (Swiss NBCN) [7], [8] and focus on Geneva–Cointrin as an example.

The focus of this paper is deliberately empirical and application-oriented. Structural properties of the index (such as mixture laws, ordering results, and connections to divergence measures between distributions) are developed elsewhere [9]. Here we emphasize the measurement principle, practical implementation, and interpretation in a climate setting.

The remainder of the paper is organized as follows. Section II introduces the regime-shift index and its empirical estimation. Section III describes the data and methodology for constructing climate regime-shift indicators. Section IV presents a case study using daily temperature data for Geneva–Cointrin. Section V discusses extensions and limitations. Section VI concludes.

## II. A Regime-Shift Index from Empirical Distributions

### A. From Powered CDFs to a Scalar Index

Let $X$ be a scalar climate variable (e.g., daily mean temperature, precipitation, or wind speed) taking values in $\mathbb{R}$, and let $F$ denote its cumulative distribution function under the *observed* climate regime. Suppose that $G$ is a reference CDF representing a baseline regime. Typical choices for $G$ include:

- a historical reference period (e.g., 1961–1990 World Meterological Organization (WMO) climate normals) [10],
- a preindustrial baseline,
- a model-simulated distribution under a policy scenario (e.g., CH2018 projections) [11].

We assume that $G$ is strictly increasing on its effective support and takes values in $(0, 1)$ there.

For any scalar $r > 0$, define the powered CDF

$$G^r(x) = \big(G(x)\big)^r, \quad x \in \mathbb{R}. \tag{1}$$

Because $G(x) \in [0, 1]$, the function $G^r$ is also a valid CDF. When $r > 1$, one has $G^r(x) \leq G(x)$ for all $x$, so $G^r$ first-order

979-8-3315-7563-2/26/$31.00 ©2026 IEEE

stochastically dominates $G$. When $0 < r < 1$, the converse holds. Hence, the scalar $r$ may be interpreted as a *regime-shift factor*: $r > 1$ corresponds to a stochastically larger distribution than $G$, and $0 < r < 1$ to a stochastically smaller one.

Treating $G^r$ as a parametric family of models, we can regard $F$ as the "true" but unknown distribution and ask which exponent $r$ best approximates $F$ within this family. Using the Kullback–Leibler divergence as the approximation criterion yields $r = R(F|G)$ as a pseudo-true exponent, which depends only on the CDF $G$ evaluated under $F$ [6], [9].

### B. Definition of Regime-Shift Functional

Let $X \sim F$. Assume $0 < G(X) < 1$ with probability 1. The *regime-shift functional* of $F$ relative to $G$ is defined as

$$R(F|G) = \left(-\mathbb{E}[\log G(X)]\right)^{-1}, \tag{2}$$

whenever the expectation is finite and strictly positive. Intuitively, $\log G(X)$ is the log of the benchmark cumulative probability assigned by the reference regime to the realized outcome; the index $R(F|G)$ rescales this expected log-likelihood and inverts it so that larger values correspond to stronger departures from the reference. The functional is inherently *relative*: if $G$ changes, then so does the interpretation of $R(F|G)$.

Several qualitative points are worth noting:

- $R(F|G) = 1$ when $F = G$, reflecting that the reference regime serves as the unit scale for itself.
- If outcomes under $F$ tend to lie in parts of the state space where $G$ assigns low cumulative probability, then $\mathbb{E}[\log G(X)]$ is more negative and $R(F|G)$ is larger, indicating a stronger shift away from the baseline.
- If outcomes under $F$ are concentrated in regions where $G$ assigns higher cumulative probability, then $R(F|G) < 1$.

**Remark 1 (Rank-Based Nature).** The index $R(F|G)$ depends on the distribution of $G(X)$ under $F$. If $T : \mathbb{R} \to \mathbb{R}$ is strictly increasing and $Y = T(X)$, with corresponding CDFs $F_Y$ and $G_Y$, then $G_Y(Y) = G(X)$ almost surely. Hence, $R(F_Y|G_Y) = R(F|G)$. This invariance under strictly increasing transformations implies that the regime-shift index remains unaffected by the choice of units (e.g., temperature in °C vs. °F).

**Remark 2 (Comparison).** Classical goodness-of-fit criteria such as the Cramér–von Mises or Kolmogorov–Smirnov statistics quantify distributional discrepancies for hypothesis-testing purposes rather than to define a scale [12]. By contrast, the RSI yields a calibrated, interpretable shift factor rather than a p-value or rejection metric.

### C. Empirical Estimator

Let $X_1, \ldots, X_n$ be independent observations of the climate variable under the regime represented by $F$ (e.g., daily temperatures in a given year or decade for a particular location). Suppose the reference CDF $G$ is known or estimated from data on a baseline period. The *empirical regime-shift index* is

$$\hat{R}_n(F|G) = \left(-\frac{1}{n}\sum_{i=1}^{n} \log G(X_i)\right)^{-1}, \tag{2'}$$

under the convention that the sum is negative and finite. No density estimation is required; only the values of $G$ at the observed points matter.

If $F$ is generated by a member of the powered family $\{G^r : r > 0\}$, one can show that $\hat{R}_n(F|G)$ coincides with the maximum-likelihood estimator of $r$ and converges to the true exponent as $n \to \infty$ [9]. More generally, $\hat{R}_n(F|G)$ converges to $R(F|G)$ in Eq. (2) by the law of large numbers [13].

## III. Data and Methodology

### A. Data Source and Variable Definition

Our empirical illustration uses daily mean temperature at Geneva–Cointrin (station code GVE), provided by MeteoSwiss as part of its Open Government Data (OGD) offering for homogeneous climate station series [7], [14]. The data stem from the Swiss National Basic Climatological Network (Swiss NBCN), which comprises long, high-quality time series that have been quality-controlled and homogenized using documented procedures [8].

Specifically, we use the historical daily data file `ogd-smn_gve_d_historical.csv`, which contains the homogeneous series of daily station observations for Geneva–Cointrin. The variable of interest is the daily mean air temperature at 2 m height above ground, denoted `tre200d0` in the OGD convention. After parsing the station abbreviation, timestamp, and temperature column, removing missing values, and restricting to complete days, the resulting sample consists of

$$N = 58{,}798$$

daily observations from 1 January 1864 to 31 December 2024. No further transformation (such as de-seasonalization, anomaly construction, or scaling) is applied; the regime-shift index is computed directly from the raw daily mean temperature in °C.

### B. Choice of Baseline and Reference CDF

We adopt the 1961–1990 period as our reference regime, in line with WMO climate normals [10] and common European practice [15], [16]. Let $\mathcal{T}_0$ denote all calendar days between 1 January 1961 and 31 December 1990. The baseline sample consists of all daily mean temperatures

$$\{X_t : t \in \mathcal{T}_0\}, \quad N_0 = |\mathcal{T}_0| = 10{,}958.$$

The empirical reference CDF is

$$\hat{G}_0(x) = \frac{1}{N_0}\sum_{t \in \mathcal{T}_0} \mathbf{1}_{\{X_t \le x\}}, \quad x \in \mathbb{R}.$$

In the implementation, $\hat{G}_0$ is obtained via MATLAB's `ecdf` routine, which returns a stepwise CDF defined on the support of the baseline sample. For the regime-shift computation we evaluate $\hat{G}_0$ at later observations using left-continuous ("previous") interpolation and truncate values to the open interval $(\varepsilon, 1-\varepsilon)$ with a small $\varepsilon$ (here $\varepsilon = 10^{-4}$) so as to avoid taking the logarithm of 0 or 1:

$$G_{\text{ref}}(x) = \max\Big\{\min\big\{\hat{G}_0(x), 1-\varepsilon\big\}, \varepsilon\Big\}. \tag{3}$$

We deliberately refrain from smoothing $\hat{G}_0$ or fitting a parametric distribution. Since the index uses only the ranks implied by the baseline, the stepwise empirical CDF already captures all relevant information, and avoiding smoothing eliminates an additional modeling choice.

### C. Evaluation Periods and Aggregation

To track the evolution of the climate regime, we compute regime-shift indices for successive calendar decades. Let the full record span the years 1864–2024. We form non-overlapping decadal blocks of the form

$$[y_k, y_k + 9], \quad k \in \{1, \dots, K\},$$

starting with $y_1 = 1864$ and ending with the last block that lies entirely within the sample (here $K = 16$, so the final full decade is 2015–2024). For each block $k$ we collect all daily temperatures

$$\{X_t : t \in \mathcal{T}_k\},$$

where $\mathcal{T}_k$ contains all days between 1 January $y_k$ and 31 December $(y_k + 9)$, and compute the decadal regime-shift index

$$\hat{R}_k = \left( -\frac{1}{|\mathcal{T}_k|} \sum_{t \in \mathcal{T}_k} \log G_{\text{ref}}(X_t) \right)^{-1}. \tag{4}$$

Here $G_{\text{ref}}$ is the truncated baseline CDF in Eq. (3). In parallel, we compute the decadal mean temperature

$$\bar{T}_k = \frac{1}{|\mathcal{T}_k|} \sum_{t \in \mathcal{T}_k} X_t.$$

The choice of decadal aggregation trades temporal resolution for robustness. With daily data, annual indices are feasible but can be noisy due to interannual variability and the small sample size of a single year. Decades strike a balance: each block contains roughly 3,650 observations, which stabilizes the empirical average in Eq. (4) while still resolving multi-decadal trends. In Section IV, we plot both $\bar{T}_k$ and $\hat{R}_k$ against the mid-decade year $y_k + 4.5$ (cf. Fig. 2).

### D. Uncertainty and Serial Dependence

The regime-shift index is an empirical functional of the observed daily data. For a decade, the effective sample size is large enough that sampling variability of $\hat{R}_k$ is modest, but it remains meaningful to acknowledge uncertainty. Standard tools from climate statistics apply here [13].

If desired, confidence intervals for $\hat{R}_k$ can be obtained via a nonparametric block bootstrap: resample blocks of consecutive days within the decade and recompute (4) for each resample [17], [18]. This preserves the short-range temporal dependence in daily temperature series and yields bootstrap distributions for $\hat{R}_k$. Analytical approximations based on the delta method[1] applied to $-\frac{1}{n}\sum \log G_{\text{ref}}(X_t)$ are also possible, though less straightforward to implement in practice.

Here we focus on point estimates and graphical trends; formal uncertainty quantification is deferred to future work.

[1]The delta method uses a first-order Taylor approximation to linearize a nonlinear statistic around its expectation to obtain an asymptotic distribution; see, e.g., Cramér [19, ch. 17].

## IV. Case Study: Geneva–Cointrin Temperature Regime Shifts

### A. Baseline versus Recent Decade: ECDF Comparison

As a first descriptive step, we compare the empirical distribution of daily mean temperature during the 1961–1990 reference period with that of the most recent full decade, 2015–2024, at Geneva–Cointrin. Let $F_{\text{ref}}$ and $F_{\text{last}}$ denote the empirical CDFs of daily temperature for the baseline and the last decade, respectively. Figure 1 plots these two ECDFs.

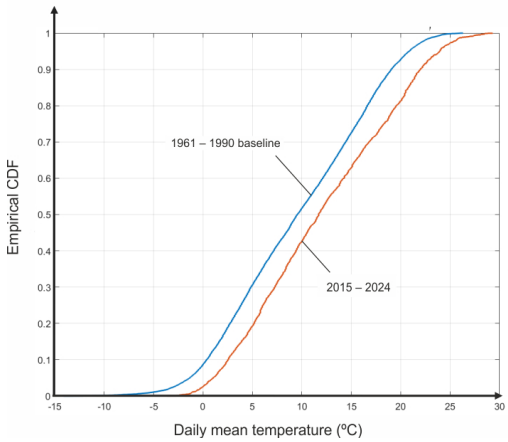



Fig. 1. Empirical CDFs of daily mean temperature at Geneva–Cointrin (GVE). Solid line: baseline period 1961–1990. Dashed line: last full decade in the sample (2015–2024). Data: MeteoSwiss homogeneous climate station series for Geneva–Cointrin (variable `tre200d0`).

The last-decade CDF is shifted to the right over virtually the entire temperature range and exhibits a thinner lower tail and a fatter upper tail than the baseline. This reflects a warmer and more extreme temperature regime: cold days (e.g., below 0°C) are less frequent than in 1961–1990, while warm and hot days (e.g., above 25°C) are more common. These shifts are consistent with independent assessments of warming and changes in extremes in Switzerland [8], [11].

### B. Decadal Mean-Temperature Trajectory and RSI

For each decade $k$ between 1864–1873 and 2015–2024, we compute the decadal mean temperature $\bar{T}_k$ and the regime-shift index $\hat{R}_k$ relative to the 1961–1990 baseline, using Eq. (4). Figure 2 shows both series as functions of the decade midpoint.

Two features stand out. First, the decadal mean temperature increases steadily over the historical record, with an approximate rise of 2°C from the earliest complete decades to the most recent one. This trend aligns with nationwide warming estimates for Switzerland [11]. Second, the regime-shift index $\hat{R}_k$ also rises over time, from values close to 1 in the early decades (indicating distributions similar to the baseline) to values near 1.4 in the most recent decade.

Before the 1961–1990 baseline itself, the decadal RSI values remain close to unity. For the pre-reference decades with sufficient data coverage, mid-decade values lie between about 0.93 (around the 1885 decade midpoint) and 1.06 (around

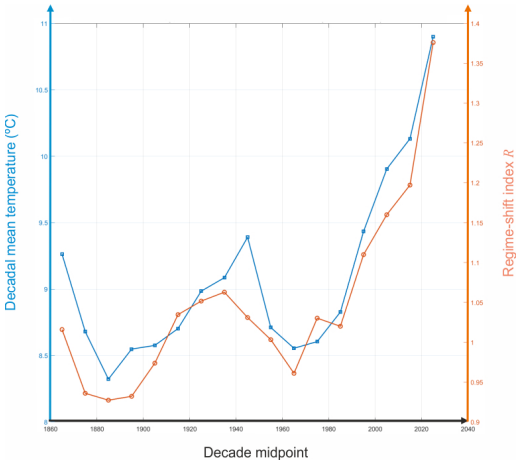



Fig. 2. Decadal mean daily temperature (left axis, squares) and RSI $\hat{R}_k$ (right axis, circles) for Geneva–Cointrin (1864–2024), relative to the 1961–1990 baseline. Each point summarizes daily mean temperatures in a decade.

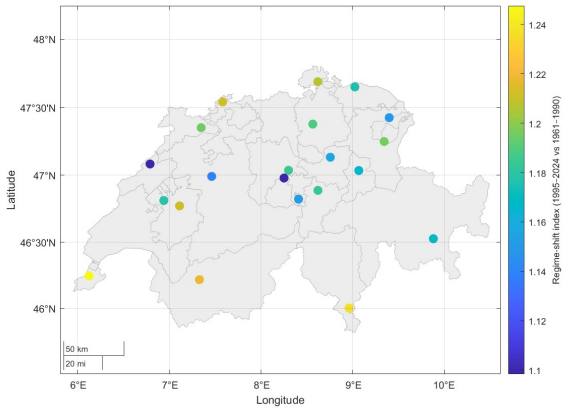



Fig. 3. Spatial RSI distribution across Switzerland, based on one representative weather station per canton (26 in total). The index compares 1995–2024 daily mean temperatures with the 1961–1990 baseline at each station.

1935). This behavior suggests a regime fluctuating around the eventual baseline distribution, without sustained directional drift. Modest deviations of RSI from 1 in this early period likely reflect sampling error and natural interdecadal variability rather than structural change.

Recall that $R(F|G)$ quantifies how much the reference CDF $G$ must be "rescaled" to approximate the observed distribution $F$ in a Kullback–Leibler sense. Higher values of $\hat{R}_k$ therefore indicate that daily temperatures are increasingly concentrated in regions where the baseline assigns relatively low cumulative probability. In this sense, the recent regime deviates more strongly from mid-century conditions: the system now spends more time in states that would have been considered relatively unusual under 1961–1990 conditions.

## V. Discussion

### A. Interpretation and Relation to Standard Indices

Standard climate-change diagnostics track shifts in mean temperature, variance, or the frequency of threshold exceedances (e.g., the ETCCDI indices for hot days,[2] warm nights, and heatwave duration) [4], [5], [20]. The regime-shift index introduced here offers a complementary perspective:

- It is *distributional*: it incorporates all quantiles of the temperature distribution, not just central moments or tail indicators.
- It is *rank-based*: it depends only on the distribution of $G(X)$, making it invariant under monotone transformations and robust to the choice of physical units.
- It is explicitly *relative*: it compares an observed regime $F$ to a specified baseline $G$, rendering the benchmark explicit and interpretable in terms of historical or policy-relevant conditions.

In the Geneva–Cointrin example, the RSI succinctly encodes how far daily temperatures have departed from a mid-20th-century regime aligned with WMO climate normals.

[2]ETCCDI: Expert Team on Climate Change Detection and Indices.

### B. Spatial Comparisons and Mapping

Beyond time series at a fixed location, the regime-shift index can be computed across many grid cells or stations, using either a common baseline $G$ or location-specific baselines $G_\ell$. The Swiss NBCN and related datasets [7], [14] are well suited for such analyses, as they provide homogeneous daily series for a dense network of long-running stations (e.g., to control for cross-sectional variation). For each station $\ell$ and period $k$, one may compute $R(F_{\ell,k}|G_{\ell,0})$ and map the resulting values to highlight spatial patterns of regime shifts.

Since altitude is a natural candidate driver of cross-sectional differences, we regress station-level RSI on station altitude across the 26 cantonal stations used in Fig. 3. The estimated relationship is modest and statistically insignificant; see Appendix B for details.

At the European scale, similar spatial analyses can be conducted with gridded datasets such as the E-OBS fields,[3] derived from the European Climate Assessment & Dataset (ECA&D) station network [15], [21]. The scalar nature of the index lends itself to spatial visualization and integration into risk dashboards for adaptation planning.

### C. Extensions to Other Variables and Multivariate Settings

Although the case study focuses on daily mean temperature, the same construction applies to:

- daily precipitation amounts, where $G$ may be a baseline rainfall distribution [13], [22];
- drought lengths or dry-spell durations, where $X$ represents the number of consecutive dry days;
- wind speeds, relevant for storm risk or wind-energy modeling.

Extension to multivariate settings (e.g., pairs $(X_1, X_2)$ such as temperature and humidity) would require working with joint distributions and multivariate CDFs, but the rank-based logic

[3]E-OBS: European land-only gridded OBServational dataset.

remains applicable. In principle, copula-based constructions could define multivariate indices that capture shifts in both marginal behavior and dependence structure.

### D. Limitations and Practical Considerations

Several limitations should be noted:

- The index is *relative* to a chosen baseline; a poorly chosen baseline can obscure or exaggerate regime shifts. Using WMO normals or other carefully justified references is therefore important [10].
- The index reduces a distribution to a single number; it does not replace a detailed analysis of specific quantiles or extremes and does not distinguish between changes in mean, variance, or tail behavior [22].
- Serial dependence and nonstationarity in daily data can affect the interpretation of $\hat{R}_k$, especially for short periods or highly autocorrelated variables [13]. Block bootstrapping or explicit time-series models can be used if formal uncertainty quantification is required [17], [18].
- The regime-shift index is univariate; joint shifts across variables (e.g., compound heat and drought events) call for additional tools [2], [3].

These caveats are common to many climate indices and call for careful integration of RSI-based summaries with more detailed statistical diagnostics and physical understanding of the climate system.

## VI. Conclusion

This paper proposes a simple, distribution-based regime-shift index for quantifying how climate regimes depart from a reference distribution. Defined at the CDF level, the index can be computed from empirical data using a closed-form expression that depends only on the reference CDF evaluated at observed outcomes. Being rank-based and explicitly relative to a baseline, the index is robust to monotone transformations and directly interpretable in terms of departures from historical or policy-relevant regimes.

The case study for Geneva–Cointrin illustrates how regime-shift indices can be computed for successive decades, yielding concise, one-number summaries of how the temperature distribution has evolved relative to the 1961–1990 baseline. The resulting trajectory tracks rising mean temperatures and reflects a growing concentration of daily states in parts of the distribution that were relatively rare under mid-century conditions.

Future work may integrate regime-shift indices with predictive climate models, use them as targets for adaptation planning, and extend them to multivariate and spatially correlated settings. In particular, combining regime-shift indices for temperature, precipitation, and wind may offer a unified, distribution-based view of environmental change at scales relevant to infrastructure design and climate-risk planning [1], [23], [24].

## Appendix A
## Geneva–Cointrin Time Series

For completeness, we summarize here the basic characteristics of the Geneva–Cointrin series analyzed in Section IV. The homogeneous daily mean temperature series (variable `tre200d0` in `ogd-smn_gve_d_historical.csv`) spans

1 January 1864 to 31 December 2024,

with

$$N = 58{,}798$$

daily observations after the removal of missing values and incomplete days. The 1961–1990 baseline subset contains $N_0 = 10{,}958$ days, and the recent 2015–2024 decade comprises $N_{\text{last}} = 3{,}652$ days. These samples are used to construct the empirical baseline CDF $G_{\text{ref}}$ and the decadal RSI values plotted in Fig. 2, as well as the ECDF comparison in Fig. 1.

## Appendix B
## Station Network and Cross-Sectional Analysis

This appendix documents the station network used in the Swiss application of the regime-shift index (RSI). One long-term station was selected per canton, using the MeteoSwiss homogeneous climate station series ("SMN, Homogeneous data") from the Swiss National Basic Climatological Network (Swiss NBCN). For each station, the RSI is computed for the recent period 1995–2024 relative to the 1961–1990 baseline, using daily mean temperature (`tre200d0`) as input.

The RSI used in the table below is the empirical estimator

$$\widehat{R}(F_{\text{rec}} \mid G_{\text{base}}) = \left( -\frac{1}{n_{\text{rec}}} \sum_{t \in \mathcal{T}_{\text{rec}}} \log G_{\text{base}}(X_t) \right)^{-1},$$

where $G_{\text{base}}$ is the empirical CDF of daily mean temperature during 1961–1990, $\{X_t : t \in \mathcal{T}_{\text{rec}}\}$ are daily temperatures in 1995–2024, and $n_{\text{rec}} = |\mathcal{T}_{\text{rec}}|$. Stations need to have at least 10 years of valid daily data in both the baseline (1961–1990) and recent (1995–2024) periods for the RSI to be reported.

For cantons with missing RSI values (AG, BL, SO, ZG), the corresponding stations did not meet the minimum data-length requirement in the 1961–1990 baseline period. Appenzell Ausserrhoden (AR) and Appenzell Innerrhoden (AI) share the same high-mountain station Säntis, which serves as a proxy for both half-cantons.

[4]BUS: Buchs/Aarau; SAE: Säntis; BAS: Basel/Binningen; RUE: Rünenberg; BER: Bern/Zollikofen; GRA: Fribourg/Grangeneuve; GVE: Genève/Cointrin; GLA: Glarus; SAM: Samedan; DEM: Delémont; LUZ: Luzern; CDF: La Chaux-de-Fonds; PIL: Pilatus; ENG: Engelberg; SHA: Schaffhausen; EIN: Einsiedeln; GRE: Grenchen; STG: St. Gallen; LUG: Lugano; HAI: Salen-Reutenen; ALT: Altdorf; PAY: Payerne; SIO: Sion; CHZ: Cham; SMA: Zürich/Fluntern. SAE serves as the proxy station for both Appenzell Ausserrhoden (AR) and Appenzell Innerrhoden (AI).

TABLE I
Swiss cantonal stations and regime-shift index (RSI) for 1995–2024 vs. 1961–1990. Stations with insufficient baseline data are indicated by "–".

| Canton | Station | Alt. (m) | RSI | Mean 61–90 | Mean 95–24 |
|---|---|---|---|---|---|
| AG | BUS | 387 | – | – | – |
| AR | SAE | 2501 | 1.197 | -1.78 | -0.51 |
| AI | SAE | 2501 | 1.197 | -1.78 | -0.51 |
| BS | BAS | 316 | 1.212 | 9.70 | 11.19 |
| BL | RUE | 611 | – | – | – |
| BE | BER | 553 | 1.140 | 8.68 | 9.67 |
| FR | GRA | 651 | 1.211 | 8.10 | 9.54 |
| GE | GVE | 411 | 1.248 | 9.63 | 11.33 |
| GL | GLA | 517 | 1.165 | 8.26 | 9.48 |
| GR | SAM | 1709 | 1.170 | 1.24 | 2.55 |
| JU | DEM | 439 | 1.195 | 8.60 | 10.02 |
| LU | LUZ | 454 | 1.185 | 9.09 | 10.32 |
| NE | CDF | 1017 | 1.098 | 6.51 | 7.27 |
| NW | PIL | 2105 | 1.099 | 1.70 | 2.49 |
| OW | ENG | 1036 | 1.150 | 5.87 | 7.02 |
| SH | SHA | 438 | 1.208 | 8.65 | 10.12 |
| SZ | EIN | 911 | 1.157 | 6.18 | 7.35 |
| SO | GRE | 428 | – | – | – |
| SG | STG | 776 | 1.149 | 7.82 | 8.94 |
| TI | LUG | 273 | 1.237 | 11.89 | 13.21 |
| TG | HAI | 719 | 1.176 | 7.44 | 8.73 |
| UR | ALT | 438 | 1.184 | 9.27 | 10.51 |
| VD | PAY | 490 | 1.178 | 8.71 | 10.02 |
| VS | SIO | 482 | 1.218 | 9.30 | 10.96 |
| ZG | CHZ | 443 | – | – | – |
| ZH | SMA | 556 | 1.189 | 8.70 | 10.04 |

*Note:* Station identifiers follow the standard MeteoSwiss three-letter codes.[4] RSI values are computed for 1995–2024 relative to the 1961–1990 baseline using daily mean temperature (`tre200d0`).

### *Regression of RSI on Station Altitude*

To assess whether altitude alone explains a substantial share of the cross-sectional variation in RSI, we estimated a simple linear regression of the form

$$\mathrm{RSI}_\ell = \beta_0 + \beta_1 \,\mathrm{Alt}_\ell + \varepsilon_\ell,$$

where $\mathrm{RSI}_\ell$ denotes the station-level regime-shift index for 1995–2024 relative to 1961–1990 and $\mathrm{Alt}_\ell$ is the station altitude in meters above sea level. The regression uses the 22 stations with valid RSI estimates and altitude information (i.e., excluding cantons with insufficient baseline data).

In this specification, the estimated slope is $\beta_1 \approx -1.8\times10^{-5}$ per meter, with a standard error of about $1.2 \times 10^{-5}$ and a two-sided $p$-value of approximately $0.14$. The corresponding coefficient of determination is $R^2 \approx 0.11$, so altitude accounts for only about 10% of the cross-sectional variance in RSI. A 1000 m difference in altitude would, under this linear approximation, be associated with a change in RSI of roughly $-0.018$, but the uncertainty around this estimate is such that the effect is not statistically significant at conventional levels.

These results suggest that, within the present network of Swiss NBCN stations, altitude by itself is at most a weak explanatory variable for the observed differences in RSI across cantons. Other factors (such as regional climate setting, exposure, or local land use) are likely to account for most of the remaining variation.

## REFERENCES


[1] IPCC, *Climate Change 2021: The Physical Science Basis*, Working Group I Contribution to the Sixth Assessment Report of the Intergovernmental Panel on Climate Change. Cambridge, UK: Cambridge Univ. Press, 2021.

[2] S. I. Seneviratne *et al.*, "Changes in climate extremes and their impacts on the natural physical environment," in *Managing the Risks of Extreme Events and Disasters to Advance Climate Change Adaptation (SREX)*, in: C. B. Field *et al.*, Eds. Cambridge, UK: Cambridge Univ. Press, 2012, pp. 109–230.

[3] C. B. Field *et al.*, Eds., *Managing the Risks of Extreme Events and Disasters to Advance Climate Change Adaptation*. Cambridge, UK: Cambridge Univ. Press, 2012.

[4] L. V. Alexander *et al.*, "Global observed changes in daily climate extremes of temperature and precipitation," *J. Geophys. Res.*, vol. 111, art. D05109, pp. 1–22, Mar. 2006.

[5] M. G. Donat *et al.*, "Updated analyses of temperature and precipitation extreme indices since the beginning of the twentieth century: The HadEX2 dataset," *J. Geophys. Res. Atmos.*, vol. 118, no. 5, pp. 2098–2118, Mar. 2013.

[6] S. Kullback and R. A. Leibler, "On information and sufficiency," *Ann. Math. Stat.*, vol. 22, no. 1, pp. 79–86, Mar. 1951.

[7] MeteoSwiss, "Swiss National Basic Climatological Network (Swiss NBCN)," Federal Office of Meteorology and Climatology MeteoSwiss, Zurich, Switzerland, documentation (in German), accessed Nov. 2025. [Online]. Available: https://www.meteoswiss.admin.ch

[8] M. Begert, T. Schlegel, and W. Kirchhofer, "Homogeneous temperature and precipitation series of Switzerland from 1864 to 2000," *Int. J. Climatol.*, vol. 25, no. 1, pp. 65–80, Jan. 2005.

[9] T. A. Weber, "A rank-based measure of distributional shifts," École Polytechnique Fédérale de Lausanne, Lausanne, Switzerland, 2025.

[10] WMO, *Guidelines on the Calculation of Climate Normals*, No. 1203, World Meteorological Organization, Geneva, Switzerland, 2017.

[11] National Centre for Climate Services (NCCS), *CH2018 – Climate Scenarios for Switzerland*. Zurich, Switzerland: NCCS, 2018.

[12] M. A. Stephens, "Tests based on EDF statistics," in R. B. D'Agostino and M. A. Stephens, Eds., *Goodness-of-Fit Techniques*. New York, NY: Marcel Dekker, 1986, pp. 97–193.

[13] D. S. Wilks, *Statistical Methods in the Atmospheric Sciences*, 4th ed. Amsterdam, The Netherlands: Elsevier, 2019.

[14] MeteoSwiss, "Climate stations – Homogeneous data series (Open Government Data)," Federal Office of Meteorology and Climatology MeteoSwiss, Zurich, Switzerland, 2025, dataset documentation, accessed Nov. 2025. [Online]. Available: https://opendatadocs.meteoswiss.ch/c-climate-data/

[15] A. M. G. Klein Tank *et al.*, "Daily dataset of 20th-century surface air temperature and precipitation series for the European Climate Assessment," *Int. J. Climatol.*, vol. 22, no. 12, pp. 1441–1453, Oct. 2002.

[16] J. Hansen, R. Ruedy, M. Sato, and K. Lo, "Global surface temperature change," *Rev. Geophys.*, vol. 48, no. 4, art. RG4004, pp. 1–29, Dec. 2010.

[17] A. C. Davison and D. V. Hinkley, *Bootstrap Methods and Their Application*. Cambridge, UK: Cambridge Univ. Press, 1997.

[18] B. Efron and R. J. Tibshirani, *An Introduction to the Bootstrap*. New York, NY: Chapman and Hall, 1993.

[19] H. Cramér, *Mathematical Methods of Statistics*. Princeton, NJ: Princeton University Press, 1946.

[20] X. Zhang *et al.*, "Indices for monitoring changes in extremes based on daily temperature and precipitation data," *WIREs Clim. Change*, vol. 2, no. 6, pp. 851–870, Nov. 2011.

[21] N. Hofstra, M. Haylock, M. New, and P. D. Jones, "Testing E-OBS European high-resolution gridded data set of daily precipitation and surface temperature," *J. Geophys. Res.*, vol. 114, art. D21101, pp. 1–16, Dec. 2009.

[22] S. Coles, *An Introduction to Statistical Modeling of Extreme Values*. London, UK: Springer, 2001.

[23] C. Folke, "Resilience: The emergence of a perspective for social–ecological systems analyses," *Glob. Environ. Change*, vol. 16, no. 3, pp. 253–267, Aug. 2006.

[24] C. S. Holling, "Resilience and stability of ecological systems," *Annu. Rev. Ecol. Syst.*, vol. 4, pp. 1–23, Nov. 1973.